J Forensic Sci, July 2009, Vol. 54, No. 4
doi: 10.1111/j.1556-4029.2009.01074.x
Available online at: www.blackwell-synergy.com

TECHNICAL NOTE

Pierre Barrier,[1,2] *M.D.; Fabrice Dedouit,*[1,2,3] *M.D.; José Braga,*[2] *Ph.D.; Francis Joffre,*[1] *M.D., Ph.D.; Daniel Rougé,*[2,3] *M.D., Ph.D.; Hervé Rousseau,*[1] *M.D., Ph.D.; and Norbert Telmon,*[2,3] *M.D., Ph.D.*

Age at Death Estimation Using Multislice Computed Tomography Reconstructions of the Posterior Pelvis*

ABSTRACT: Thanks to recent advances, computed tomography is now seen as a tool of great value in the field of physical anthropology. In this study, we focused on the posterior pelvis and the auricular surface and evaluated the accuracy of 3D reconstructions of the auricular surface, using a methodology derived from a previous study by Lovejoy et al. We also looked for trabecular bone criteria expressing age-related changes. Forty-six coxal bones were scanned, and scoring of macroscopic criteria showed a good agreement between 3D reconstructions and photographs, especially for transverse organization ($k = 0.90$). The changes occurring in the posterior part of the sacropubic trabecular bundle were evaluated on CT reconstructions via three new criteria, which exhibited a good intra- and inter-observer agreement ($k = 0.77–0.89$), and were particularly useful in identifying older subjects. We concluded that these CT-evaluated trabecular bone criteria are promising and yield useful information about age at death.

KEYWORDS: forensic science, forensic anthropology, bone age determination, posterior pelvis, auricular surface, trabecular bone, multislice computed tomography

Estimating age at death in forensic or paleoanthropological contexts remains one of the most challenging goals of physical anthropology. An approach combining multiple methods is often recommended to provide an accurate estimation (1,2). Among the different anatomic areas used for this purpose, the posterior pelvis is a solid bony region involved in the body load transfer supported by the sacroiliac (SI) joint, where degenerative changes continue to occur until old age (2,3). The auricular surface, defined as the subchondral bone of the iliac part of the SI joint, has been used to develop age at death estimation methods. Lovejoy's method, published in 1985, was the first attempt to use the auricular surface in estimating age at death (2,3). Typical stages of aging of the auricular surface were defined and this method is based on comparison of the specimen to modal stages. Regarded as independent of sex (4), Lovejoy's method also has the advantage of using the durable bony region supporting the auricular surface, which is often recovered in a paleoanthropological context (5). However, high intra-observer error and a tendency to overestimate ages of younger adults and underestimate ages of older individuals have been noted (6–8). To overcome these limitations, Buckberry and Chamberlain recently proposed a revised method, using an independent evaluation of each characteristic and a composite score (9). This method was initially thought to be promising, but a more recent report suggested that the results achieved by the authors may have been too optimistic, and that only three different chronological stages derived from the composite score can be statistically supported (10). This independent scoring is however regarded as easier to apply than the original method, and may confidently identify older individuals (10).

During the last two decades separating the original from the revised method, computed tomography (CT) has made major technological advances, resulting in dramatic improvement of spatial resolution and real time volume rendering as well as greater availability. Features of the auricular surface can now be evaluated on CT-based 3D reconstructions. Such volume rendering technique (VRT) reconstructions have already been used for sex determination of mummies (11), using macroscopic criteria previously established by Acsadi and Nemeskeri (12) and by Ferembach (13). More recently, Telmon et al. applied the Suchey-Brooks method to 3D reconstructions of the pubic symphysis and demonstrated similar accuracy of age at death estimation as with the original method applied to dry bones (14). In addition to cortical surface findings, high resolution CT scan also provides trabecular bone details.

On the proximal ends of long bones, trabecular bone shows an anisometric organization, with distinct bundles, previously used by Acsadi and Nemeskeri in estimating age at death (12). Coxal trabecular bone has never previously been used for this purpose. However, load transfer during the growing phase of the coxal bone results in a distinctive trabecular architecture, where several bundles may be distinguished. This relationship between bipedal gait and the distinctive pattern of human trabecular organization was studied more than half a century ago by Correnti (15), who identified three specific trabecular bundles in humans. This author observed an idiobadismatic or gait-related system of trabecular organization featuring a sacropubic bundle and an ilioischial bundle, intersecting at a chiasma. The biomechanical basis of this system has since been demonstrated (16), and Correnti's work was used in the nineties to seek arguments for the bipedal gait of fossil hominoids (17–19).

[1]Service de Radiologie Générale, Hôpital de Rangueil, Avenue du Professeur Jean Poulhès, 31403 Toulouse Cedex 4, France.
[2]Imagerie de Synthèse en Anthropobiologie, Université Paul Sabatier, FRE 2960 CNRS, 37 allées J Guesde, 31000 Toulouse, France.
[3]Service de Médecine Légale, Hôpital de Rangueil, Avenue du Professeur Jean Poulhès, 31403 Toulouse Cedex 4, France.

*Presented at the 60th Annual Meeting of the American Academy of Forensic Sciences, February 18–23, 2008, in Washington, DC.

Received 11 Feb. 2008; and in revised form 15 Sept. 2008; accepted 28 Sept. 2008.

We decided to assess the feasibility and accuracy of multislice CT (MSCT) evaluation of previously reported features of the auricular surface and to look for potentially informative data provided by trabecular bone analysis, focusing on the sacropubic bundle.

Materials and Methods

Age-related changes in the coxal bone affect both the superficial cortical bone and the underlying trabecular bone. Therefore, CT reconstructions of the auricular surface were created to show the relevance of auricular surface features assessment via CT. Beyond the cortical bone, we looked for trabecular bone criteria exhibiting age-related changes. The terminology used to describe the auricular surface is that of Lovejoy et al. (1) and Buckberry and Chamberlain (9).

Bone Collection and MSCT

We used a sample of 46 coxal bones comprising 14 female and 32 male individuals, belonging to a forensic collection. This forensic collection of known sex and age, elaborated during previous decades, belonged to a French University Hospital. The demographic structure of the reference sample is displayed on a histogram (Fig. 1). All specimens were scanned at 140 kV/200 mAs using a 16-detector scanner (Somatom Sensation 16; Siemens Medical Solutions, Erlangen, Germany) with 0.6 mm slice thickness. Overlapping slices were obtained using a bone reconstruction algorithm (B80) and used to create multiplanar (MPR) and VRT reconstructions on an Advantage Window® workstation (GE, Milwaukee). MPR views (0.6 mm slice thickness, 0.3 mm overlap) were aligned perpendicularly to the axis of each demiface of the auricular surface for examination of the trabecular bone. The transfer function used to create the VRT reconstructions assigned a total opacity for all attenuations exceeding −600 HU. This threshold was determined experimentally as a compromise between inclusion of all bone voxels and avoidance of artifacts. For comparison, digital images of every specimen were also obtained from the same angle and with tangential lighting.

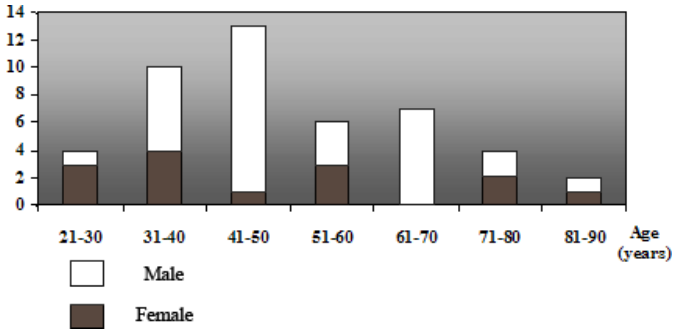

FIG. 1—*Demographic structure of the sample, by decades.*

Macroscopic Criteria

Macroscopic criteria were scored independently using a three-stage scale. These criteria were transverse organization, macroporosity, and apical activity. The stages are described in Table 1.

Macroporosity was defined as cortical perforation greater than 1 mm in diameter, exposing the cancellous bone. Care was taken to differentiate macroporosity from postmortem damage and from nutrient foramina. Transverse organization is a young feature, referring to a pattern of radial striae running perpendicularly to the axis of each demiface from one margin of the auricular surface to the other (Fig. 2). At the apex, degenerative changes were scored as three different stages of apical activity, the contour becoming smooth, and associated with osteophytic growth (lipping) with aging.

Other criteria previously used by Lovejoy et al. (1) and Buckberry and Chamberlain (9) were considered potentially informative, but were excluded after preliminary analyses of the 3D reconstructions. With regard to surface texture, the grain of the surface has to be highly simplified to be reproducible: as finely granular, coarsely granular, and dense bone are poorly distinguishable on 3D reconstructions, the surface texture as seen in 3D reconstruction was not sufficiently informative. Microporosity was not seen due to volume averaging effect.

Trabecular Bone Criteria

The trabecular bone criteria used were:

The sacropubic bundle, beneath the auricular surface cortex, was identified on MPR reconstructions as a linear organization of trabecular cells, aligned downward and forward from the auricular surface to the pubis. This bundle, obvious in young specimens (Figs. 3*a* and 3*b*) was not visible in older subjects (Figs. 4*a* and 4*b*). Visualization of the posterior part of the sacropubic bundle concentrated on the central line of the bundle and trabecular cells in contact with this line, called juxtalinear cells. The sacropubic bundle and its components correspond to the bundle previously described by Macchiarelli et al. (17).

The central line was followed from the posterior tip of the inferior demiface to the apex, where the bundle took a more vertical course, parallel to the iliac cortex in front of the great sciatic notch. Depending on its integrity, the central line was scored as continuous, discontinuous or absent. Juxtalinear cells are in direct contact with the central line and are aligned in the same direction. These

TABLE 1—*Macroscopic criteria of age at death: scoring.*

Criteria	Definition	Stages	Score
Transverse organization	Striae or billowing transversally running from the medial to the lateral margins of the auricular surface	No organization/A few isolated striae	Absent
		Moderate organization/organization affecting only one demiface	Moderate
		Obvious organization, affecting both demifaces	Marked
Macroporosity	Holes or defect greater than 1 mm in auricular surface	No porosity	Absent
		Porosity affecting one demiface, or very limited porosity affecting both demifaces	Moderate
		Extensive porosity affecting both demifaces	Marked
Apical activity	Irregularity, lipping, dull rim	Apex sharp, distinct, no degenerative changes	Absent
		Intermediate form, moderate lipping with distinct and smooth margin	Moderate
		Irregularity of contour, dull rim, marked lipping	Marked

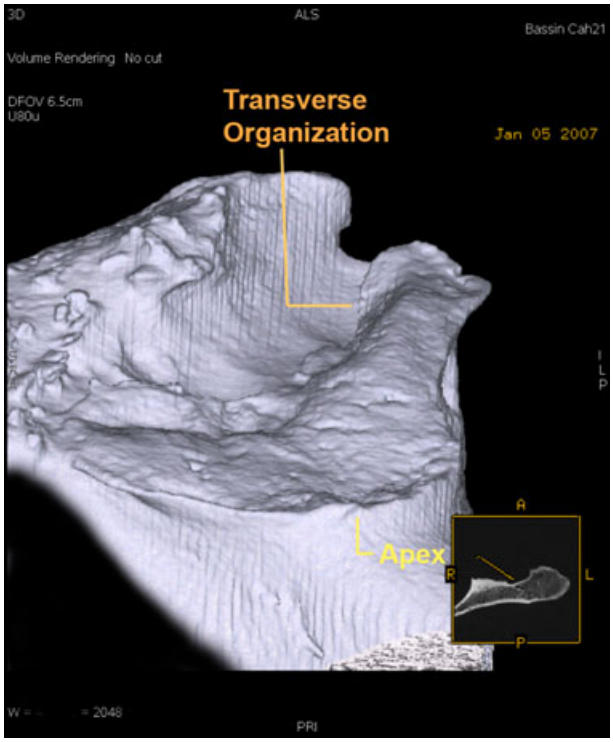

FIG. 2—*Transverse organization: radial striae as depicted on VRT reconstructions.*

cells are wider than the surrounding ones, a feature clearly distinct in younger individuals. Visualization of the juxtalinear cells was scored as absent or present. On CT images of younger individuals, trabecular bone attenuation is more marked below the bundle than above it. This results in an attenuation gradient, probably related to the diameter and number of cells, but also to trabecular thickness. This gradient tends to disappear with aging, and its visualization was scored on a three stage scale (Table 2).

Study Method and Statistical Analysis

The scoring system was used by a first observer to perform two evaluations at a 3-week interval, while a third evaluation was performed by another observer. Descriptive statistics and statistical analysis were performed with SAS/STAT® software (SAS Institute Inc., Cary, NC). Due to the small size of the sample, the Kruskal–Wallis test (nonparametric test) was used for statistical analysis. Cohen's kappa nonparametric test was used to assess intra-observer and inter-observer agreement as well as "intermodality" agreement.

Results

Accuracy and significance as well as reproducibility are shown in Tables 3, 4, and 5. The boxplots are a convenient way of graphically depicting the accuracy of the different features and allow immediate perception of the potential overlap of different stages (Figs. 5*a–f*). Main results and their interpretation are exposed in the following discussion.

Discussion

Thanks to recent technological advances, MSCT is expected to be an extremely valuable tool in the field of physical anthropology. Because of the great "natural" contrast of bone, CT can be used to transpose previously tested macroscopic features to 3D reconstructions when attempting to estimate age at death. However, its ability to provide relevant information from the trabecular bone should not be overlooked.

Of the different 3D criteria evaluated in this study, transverse organization is a young feature, allowing confident identification of specimens under 40 when it is present and marked on both demifaces. This result is in agreement with the conclusion reported by Lovejoy et al. (3). This feature demonstrated good intra- and inter-observer agreement ($k = 0.82$) and also good agreement between image-based and 3D-based evaluations ($k = 0.90$). In this study, the evaluation of porosity of the surface, corresponding to macroporosity in the original study by Lovejoy et al., provided interesting information. Due to spatial resolution limitations, partial volume artifact results in false positive macroporosity, occurring when the cortical bone is so thin that its voxel densities are lower than the threshold selected for the VRT transfer function (in this study −600 HU). However, we demonstrated good agreement between VRT reconstructions and photos ($k = 0.73$). It is likely that true porosity as observed macroscopically and a false-positive 3D artifact secondary to a very thin cortical surface are close

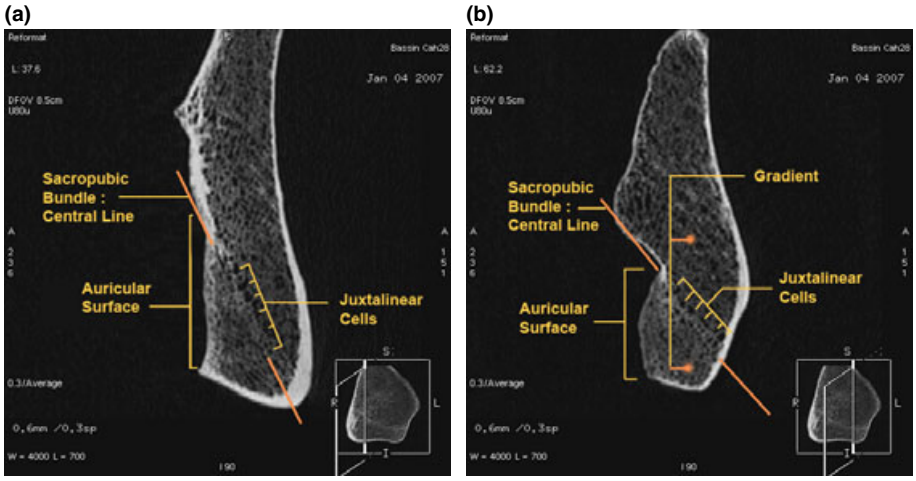

FIG. 3—*Trabecular bone architecture: young subject. (a) Central line and juxtalinear cells of the sacropubic bundle are well visualized. (b) Attenuation gradient below and above the central line is clearly seen.*

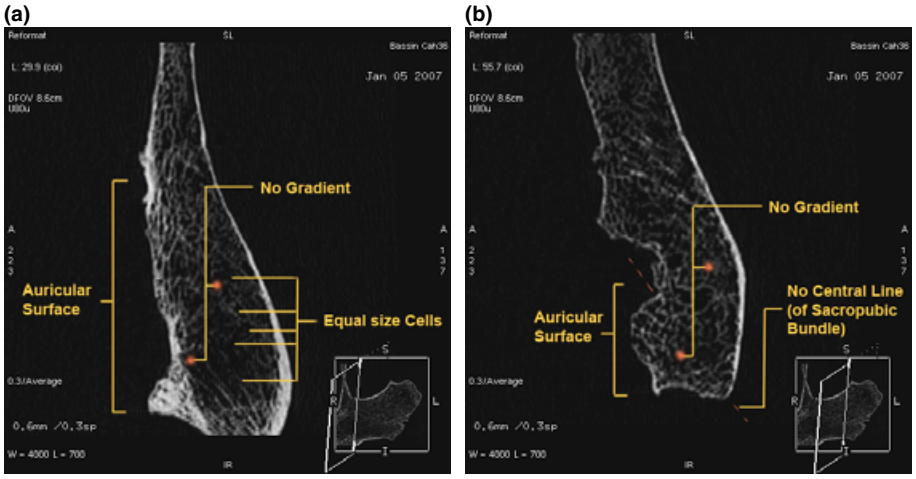

FIG. 4—*Trabecular bone architecture: older subject. (a) Central line and juxtalinear cells of the sacropubic bundle are not visible. (b) Trabecular cells are wider, of equal size, and no gradient can be highlighted.*

TABLE 2—*Trabecular bone criteria: scoring.*

Criteria	Definition	Stages and Score
Sacropubic bundle: central line	Definite line at the center of the sacropubic trabecular bundle. Running from the superior margin of the inferior demiface toward the pubic region	Continuous: visible all along the auricular surface Discontinuous Absent
Sacropubic bundle: juxtalinear cells	Rectangular or ovoid cells in contact with the central line, with a great axis parallel to the line	Present Absent: nonvisible
Attenuation gradient	Increased attenuation of the trabecular bone below the sacropubic bundle, in comparison with the area immediately above it	Marked: obvious Moderate: subtle attenuation difference Absent

TABLE 3—*Age estimation from macroscopic criteria: 3D reconstructions. Mean, standard deviation, minimum and maximum age, and statistical analysis.*

							Kruskal–Wallis Test	
Criteria	Stage	*n*	Mean	SD	Minimum	Maximum	χ^2	*p*
Transverse organization	Marked	9	33.67	12.46	24.00	65.00	14.94	0.0006
	Moderate	13	47.62	14.20	32.00	75.00		
	Absent	24	57.46	13.77	34.00	84.00		
Macroporosity	Absent	12	37.00	13.25	24.00	65.00	13.90	0.0010
	Moderate	21	49.81	11.16	32.00	68.00		
	Marked	13	62.38	16.80	32.00	84.00		
Apical activity	Absent	11	35.36	10.42	24.00	59.00	14.41	0.0007
	Moderate	21	51.52	14.39	32.00	75.00		
	Marked	14	59.29	15.17	32.00	84.00		

TABLE 4—*Age estimation from trabecular bone criteria. Mean, standard deviation, minimum and maximum age, and statistical analysis.*

							Kruskal–Wallis Test	
Criteria	Stage	*n*	Mean	SD	Minimum	Maximum	χ^2	*p*
Visualization of the sacropubic bundle: central line	Continuous	9	37.89	9.47	28.00	57.00	13.61	0.0011
	Discontinuous	20	46.00	14.50	24.00	75.00		
	Absent	17	61.18	14.48	34.00	84.00		
Visualization of the sacropubic bundle: juxtalinear cells	Present	28	42.43	13.36	24.00	75.00	14.95	0.0001
	Absent	18	61.83	13.03	43.00	84.00		
Attenuation gradient	Marked	9	37.67	11.84	28.00	59.00	13.22	0.0013
	Moderate	12	42.67	12.87	24.00	65.00		
	Absent	25	58.00	14.82	32.00	84.00		

chronological stages in the aging process. As expected, apical activity concorded well in photos and VRT reconstructions, and showed marked overlap between moderate and advanced stages.

On the basis of these findings, we conclude that spatial resolution issues still remain a drawback of CT evaluation of the auricular surface: some subtle macroscopic criteria are invisible.

TABLE 5—*Inter-observer and intra-observer variability.*

Criteria	Intra-Observer Agreement	Inter-Observer Agreement	Agreement Between c3D and Photos
Transverse organization	0.82	0.82	0.90
Macroporosity	0.83	0.65	0.73
Apical activity	0.93	0.93	0.63
Central line	0.89	0.82	NA
Juxtalinear cells	0.77	0.77	NA
Attenuation gradient	0.89	0.85	NA

Cohen's kappa coefficient.
NA, not applicable.

However, even if CT evaluation does not have analytical advantages over gross observation of dry bones, certain auricular surface features can be accurately assessed with CT. The relevant features are included in a digital data set, allowing an easy archival for later analysis. Moreover, partial analysis of the auricular surface via CT may be useful when working on fleshed bodies when disarticulation and maceration would be complicated.

Beyond the transposition of macroscopic methodology, the thin CT slices (0.6 mm) gave us the opportunity to seek and evaluate aging criteria using the trabecular bone. Acsadi and Nemeskeri previously used plain radiography of thin histological slices to describe six typical aging stages of the trabecular architecture of the proximal femur and humerus (12). The approach described by Acsadi and Nemeskeri has been applied to the coxal bone, which displays a distinctive architecture of bundles which is related to human bipedal gait. However, almost four decades ago when these authors developed their method based on plain radiography of histological slices, analysis of trabecular architecture required long and destructive preparation. Nowadays, instant and noninvasive access to trabecular bone is provided by thin slice CT studies. Among the various components of Correnti's idiobadismatic system, we chose to describe the aging process affecting the posterior part of the

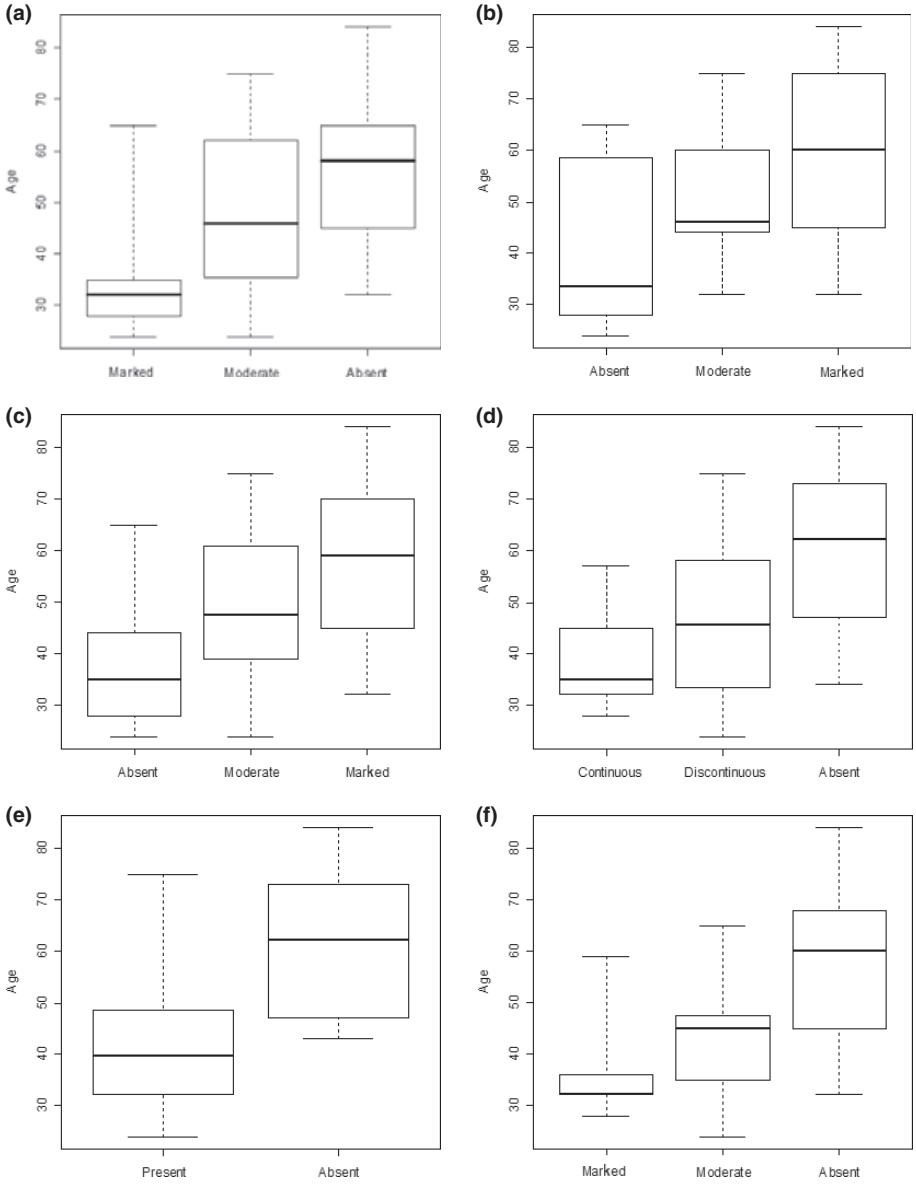

FIG. 5—*Boxplots: (a) Transverse organization. (b) Macroporosity. (c) Apical activity. (d) Central line of the sacropubic bundle. (e) Juxtalinear cells. (f) Attenuation gradient. Box represents interquartile range, black horizontal line represents median, and t-bars represent extremes.*

sacropubic bundle, which undergoes degenerative changes resulting in loss of visualization.

The integrity of the sacropubic bundle was related to the visibility of central line and juxtalinear cells of the bundle. These two features were modified with age: the association of a continuous line with visible juxtalinear cells presents almost no overlap with an absent central line and absent cells. Therefore, we found that the absence of visibility of the sacropubic bundle reliably identified subjects aged over 50 years old. This study highlights an attenuation difference of the cancellous bone on both sides of the bundle: the attenuation is more pronounced below the sacropubic bundle. This gradient is a young feature and an absent gradient is also associated with ages older than 45. A visual evaluation of the gradient has been chosen and it could be suggested that the application of an attenuation measurement in a region of interest (ROI) on CT might have been more objective. However, changes in yellow marrow fat content in the elderly are a cause of reproducibility bias in quantitative CT evaluation of osteoporosis. Moreover, the fatty content of the cells is progressively replaced by air after death, which may result in greater attenuation variability. Intra- and inter-observer agreement were good for evaluation of the gradient ($k = 0.89$ and $k = 0.85$), which supports the choice of a visual evaluation.

This study has several limitations, mainly because the sample was small and the genders were not equally represented. With such a limited sample, highlighting sex differences in age-related changes was not possible. Such differences are unlikely regarding the features evaluated on 3D reconstructions, as sexual independence has been demonstrated in several macroscopic series (4,9,20). Nonetheless, bone mineral density is affected by calcium intake and is known to decrease faster in postmenopausal women, resulting in a threefold higher fracture incidence. Therefore, the architecture of the trabecular bone and the sacropubic bundle are likely to undergo sex-related differences.

For the purpose of estimating age at death, some subtle features seen on gross analysis cannot be assessed on CT evaluation. However, virtual scoring of several macroscopic criteria can confidently be performed using MSCT VRT reconstructions, and the same set of data can provide relevant information from the analysis of the trabecular bone. The results achieved here with 16 channels CT are likely to be outstripped by the better resolution of the more recent CT scanners. One of the most interesting perspectives is the possibility of applying this method to trabecular bone in the context of virtual autopsy or *in vivo*. Segmentation of the 3D volume allows virtual dislocation of the joint, which is quick and easy for a true diarthrosis, for example the coxofemoral joint. However, in the present state of the art, this is not feasible within an acceptable scan time for the SI joint. Utilizing the advantages of picture archiving and communication systems (PACS) for medical imaging, anthropologic or forensic CT images are easy to store and to transfer, a feature useful in the victim identification process (21). Eventually, a database of CT scans of various bones of known sex and age may be created and take its place in a larger virtual anthropologic library.

Acknowledgment

Sincere appreciation is expressed to Nina Crowte for her assistance in the preparation of this manuscript.

References

1. Lovejoy CO, Meindl RS, Mensforth RP, Barton TJ. Multifactorial determination of skeletal age at death: a method and blind tests of its accuracy. Am J Phys Anthropol 1985;68:1–14.
2. Martrille L, Ubelaker DH, Cattaneo C, Seguret F, Tremblay M, Baccino E. Comparison of four skeletal methods for the estimation of age at death on white and black adults. J Forensic Sci 2007;52:302–7.
3. Lovejoy CO, Meindl RS, Pryzbeck TR, Mensforth RP. Chronological metamorphosis of the auricular surface of the ilium: a new method for the determination of adult skeletal age at death. Am J Phys Anthropol 1985;68:15–28.
4. Murray KA, Murray T. A test of the auricular surface aging technique. J Forensic Sci 1991;36:1162–9.
5. Waldron T. The relative survival of the human skeleton: implication for palaeopathology. In: Boddington A, Garland AN, Janaway RC, editors. Death, decay and reconstruction. Manchester, UK: Manchester University Press, 1987;55–64.
6. Bedford ME, Russell KF, Lovejoy CO, Meindl RS, Simpson SW, Stuart-Macadam PL. Test of the multifactorial aging method using skeletons with known ages-at-death from the Grant Collection. Am J Phys Anthropol 1993;91:287–97.
7. Saunders SR, Fitzgerald C, Rogers T, Dundar C, McKillop H. A test of several methods of skeletal age estimation using a documented archaeological sample. Can Soc Forensic Sci J 1992;30:49–60.
8. Schmitt A. Age-at-death assessment using the os pubis and the auricular surface of the ilium: a test on an identified Asian sample. Int J Osteoarchaeol 2004;14:1–6.
9. Buckberry JL, Chamberlain AT. Age estimation from the auricular surface of the ilium: a revised method. Am J Phys Anthropol 2002;119:231–9.
10. Falys CG, Schutkowski H, Weston DA. Auricular surface aging: worse than expected? A test of the revised method on a documented historic skeletal assemblage Am J Phys Anthropol 2006;130:508–13.
11. Cesarani F, Martina MC, Ferraris A, Grilletto R, Boano R, Marochetti EF, et al. Whole-body three-dimensional multidetector CT of 13 Egyptian human mummies. AJR Am J Roentgenol 2003;180:597–606.
12. Acsadi G, Nemeskeri L. History of human life span and mortality. Budapest: Akademiai Kiado, 1970.
13. Ferembach D, Schwidetzky I, Stloukal M. Recommandations pour déterminer l'âge et le sexe sur le squelette. Bull Mém Soc Anthropol Paris 1979;13:7–45.
14. Telmon N, Gaston A, Chemla P, Blanc A, Joffre F, Roug D. Application of the Suchey-Brooks method to three-dimensional imaging of the pubic symphysis. J Forensic Sci 2005;50:507–12.
15. Correnti V. Le basi morfomeccaniche della struttura dell'osso iliaco. Riv Antrop 1955;42:289–336.
16. Dalstra M, Huiskes R. Load transfer across the pelvic bone. J Biomech 1995;28:715–24.
17. Macchiarelli R, Bondioli L, Galichon V, Tobias PV. Hip bone trabecular architecture shows uniquely distinctive locomotor behaviour in South African australopithecines. J Hum Evol 1999;36:211–32.
18. Rook L, Bondioli L, Kohler M, Moyà-Solà S, Macchiarelli R. Oreopithecus was a bipedal ape after all: evidence from the iliac cancellous architecture. Proc Natl Acad Sci U S A 1999;96:8795–9.
19. Tobias PV. Ape-like australopithecus after seventy years: was it a hominid? J R Anthropol Inst 1998;4:283–308.
20. Mulhern DM, Jones EB. Test of revised method of age estimation from the auricular surface of the ilium. Am J Phys Anthropol 2005;126:61–5.
21. Sidler M, Jackowski C, Dirnhofer R, Vock P, Thali M. Use of multislice computed tomography in disaster victim identification—advantages and limitations. Forensic Sci Int 2007;169:118–28.

Additional information and reprint requests:
Pierre Barrier, M.D.
Service de Radiologie Générale
Hôpital de Rangueil
Avenue du Professeur Jean Poulhès
31403 Toulouse Cedex 4
France
E-mail: p.barrier@gmail.com